

1 *Conference Proceedings Paper*

2 **Reference system effects detected with meridian** 3 **astronomy on the Clementine Gnomon (Rome, 1702)**

4 **Costantino Sigismondi** ^{1,2,3}

5 Published: date

6 Academic Editor: name

7 ¹ ICRA/Sapienza Univeristy of Rome;

8 ² Ateneo Pontificio Regina Apostolorum, Rome;

9 ³ ITIS Galileo Ferraris, Rome

10 * Correspondence: sigismondi@icra.it

11 **Abstract:** The Clementine Gnomon was built in 1700-1702 by the astronomer Francesco Bianchini,
12 upon the will of the Pope Clement XI. This meridian line is located in the Basilica of santa Maria degli
13 Angeli e dei Martiri in Rome, and it is visited by thousands of students each year.

14 This 45 meters' meridian allows to measure the secular variation of the obliquity of the ecliptic ϵ and
15 the periodical nutation effect. Only a pencil and a meter are required to get an accuracy up to one
16 arcsecond.

17 I analyze the data from November 2020 to January 2021 with respect to the following keywords:
18 ephemerides, aberration (optical and stellar, i.e. special relativistic), nutation, proper motion,
19 precession, refraction anomalies, apsides, solstices, equinoxes, tropical year, Sun rotation, equation
20 of time, Earth rotation and DUT1, obliquity, eccentricity, air turbulence, penumbra, time accuracy,
21 ecliptic coordinates, zodiacal signs, and metrological precision. Each one of these fall-winter data are
22 in agreement with ephemerides within few arcseconds and the major sunspots have been visible in
23 the solar image projected by the lensless pinhole on the floor of the Basilica.

24 All those considerations pave the way to modern astrometry, where the sub-arcsecond accuracy is
25 required in order to detect clearly the relativistic effects.

26 **Keywords:** ephemerides; optical aberration; stellar aberration; nutation; refraction; solstices;
27 equinoxes; equation of time; Earth's rotation; obliquity; eccentricity; air turbulence; penumbra.
28

29 **1. Introduction: The Great Clementine Gnomon as in the texts of Francesco Bianchini (1703)**

30 The meridian line was completed in about two years: 1701 and 1702, including all the images of the
31 zodiacal signs and the stars over the floor. The stars are located along the projection of the celestial
32 equator, and of the projected paths (hyperbolae) of Sirius, Arcturus and of the Sun the 20th of
33 August 1702 (visit of the Pope Clement XI). Another group of 7 stars on a circular sector at 35 m 80
34 from the pinhole's base, approach the Sirius' hyperbola.

35 Francesco Bianchini published in 1703 [1] the results of the measurements made at the meridian line
36 in the book *De Nummo et Gnomone Clementino*, and the four instants of solstices and equinoxes (*anni*

37 *cardines*)- were written on a marble slab included in the wall of the presbyterium, at about five
38 meters from the Capricorn sign.

39 Bianchini called the great meridian line *Clementine Gnomon*, because with this instrument, dedicated
40 to Clement XI, it is possible “to know” the position of the Sun. The word Gnomon includes the
41 Greek root for knowledge, knowing.

42 **2. Measurements and comparison with ephemerides**

43 **2.1.1 Ephemerides for 1703**

44 IMCCE provides a service for computing the beginning of the seasons back to year 4000 BC. I refer
45 to these computations, which are not available in NASA web interface Horizons (only back to 1800
46 AD).

47 The comparison between IMCCE UTC dates and Bianchini measurements, in local time, requires
48 also to “translate” local time of 1703 into UTC with a slightly different equation of time with respect
49 to the present time, as well as different position of the apsides of the Earth (Sun) orbit.

50

51 **2.1.2 Aberration in stellar coordinates**

52 Bianchini measured the difference of time between the transits of the Sun and the transit of Sirius.
53 He measured this difference in daylight also during the solstice of June, as reported in his book, so
54 there is no doubt he did it also during the Sirius’ night transit in December, and in twilight at both
55 equinoxes. The Stars’ Catalogue published in 1700 by Philippe de la Hire (Paris Royal Observatory)
56 was used by Bianchini, and on the meridian line the coordinates “precessed” for 1701 have been
57 written [2-3].

58 While the stellar coordinates in the Catalogue were carefully measured at night with a “passages
59 instrument” i.e. a meridian instrument, the observation in daylight deals with the aberrated
60 coordinates of the same star, and the noon transit of a star carries a difference of 40”, the double of
61 aberration’s amplitude, being the star’s position 6 months after the midnight (opposition) transit.

62 The differences between IMCCE ephemerides and Bianchini’s calculated times reflects the influence
63 of the aberration of stellar coordinates, not included in Bianchini’s computations.

64

65 **2.1.3 Polaris’ stellar aberration**

66 Bianchini could not take into account of stellar aberration, because it was discovered in 1727 by
67 James Bradley, but he observed and measured its effects. The first of them was in the latitude that
68 he measured during the nights from 1 to 8 January 1701 by averaging the extremes of the altitude of
69 Polaris. He obtained $41^{\circ} 54' 27''$ while the correct value is 16” less. This difference is due to the
70 stellar aberration of the Polaris coordinates in these dates. Note that his measurements was
71 independent from the coordinates of the Polaris, depending only on the observations [3].
72 The stellar aberration is a special relativistic effect measurable with the Clementine Gnomon.

73

74 **2.1.4 Bianchini effect on Sirius**

75 Bianchini observed the change of the meridian coordinates of Sirius along the seasons with a
76 telescope, whose axis was on the meridian line. Over the pinhole of Santa Maria degli Angeli a
77 window 40 cm x 60 cm was opened to allow these observations. Nowadays (2021) it cannot be done
78 anymore, without taking the risk to break the coat of arms of Clement XI in which the pinhole is
79 located.

80 Bianchini measured in 1701-1702 a difference of 0.1 centesimal parts in the meridian coordinate of
81 the projection of Sirius along the year: the tangent of its observed zenithal angle changed from
82 1.6138 to 1.6128 with a difference of nearly 1' =60" **from night** (December) **to day** (June). It has been
83 the first time in literature that seasonal refraction effects are accounted. That's why I call it the
84 *Bianchini effect*. To observe it on the solar positions I managed to calibrate the meridian line (and the
85 present pinhole position) up to 1 mm of accuracy, but no evident effect >10" has ever been noticed
86 in the O-C, Observed-Calculated positions of the solar limbs, in more than two years (2018-2021).

87 The aberration ellipse for Sirius has semiaxis k and $k \cdot \sin(\beta)$ with $k=20.5''$ and $\beta=-39.5^\circ$; the meridian
88 maximum shifts are $\pm k \cdot \sin(\beta)=\pm 13''$ near the equinoxes. Bianchini observed the maxima in July 1702
89 and the minima in January-March 1702. In the following table (Bianchini, 1703 [1]) we see dates
90 and tangents of zenithal angle of Sirius ($\times 100000$).

<i>Anno</i>	<i>Die</i>	<i>Mense</i>	
1702.	1	Augusti	partes 161340.
	8	Augusti	———— 161358.
	23	Septembris	———— 161330.
1703.	8	Januarii	———— 161280.
	3	Februarii	———— 161280.
	14	Martii	———— 161280.
	12	Maii	———— 161320.
	11	Julii	———— 161380.

91 Table 1. Meridian observations of Sirius by Francesco Bianchini at the Clementine Gnomon, also in daylight.
92
93



94 **Figure 1.** The image of the Sun entering the Aquarius on January 19, 2021
95

96 **2.2. The winter solstice of 2020, in comparison with 1703**

97 Now (2020) the position of the Southern solar limb, on the meridian line, exceeds the number 220
98 only from 19 to 23 December, and it reached +45 mm on 21st (included the penumbra). During 1701
99 the solar limb touched the black line contour of the Capricorn (CAP), at the end of the meridian
100 line, +128 mm above 220 mark.

101 **2.2.1 Solstices' parabola, obliquity and nutation**

102 During the solstices, the solar declination reaches an extreme and inverts its growth, through a
103 stationary point. Around this stationary point the meridian coordinates (the tangent of the observed
104 zenithal angle either of the center of the Sun, either of both solar limbs) behave in time like a
105 parabola, centered in the instant of the solstice. The fit of the parabola gives the minimum's instant
106 and its position (declination + refraction + nutation [7-8]). The nutation is an oscillation of $\pm 9''$ in 18
107 years, which correspond to ± 4.5 mm at the winter solstice on the Clementine Gnomon. The accuracy
108 of a solar limb position is within ± 1 mm, and the fit of a whole week of data reaches a better
109 precision on the minimum of the parabola.

110 **2.2.2. Winter solstice 2020 instant from the position of the limbs**

111 The instant of the minimum, averaged from Southern and Northern limbs between 7 December and
112 4 January, is 21 December at 10:37 \pm 4 min. The time of the solstice in IMCCE ephemerides is at 11:02
113 TMEC, 25 minutes later. The causes of this difference are not dependent on the calibration of the
114 meridian line, since the position of the limbs can be measured from each of the references on the
115 line: the "tropic", i.e. the inversion of the motion, is universal.

116 **Table 2.** Southern and Northern solar limb's positions on the meridian line, measured from its end.

Date [December 2020]	Southern limb [mm]	Northern limb [mm]
7,50138	1618	2661
10,50232	1041	2111
11,50263	879,5	1953
13,50329	595	1687
14,50362	478	1570,5
17,50463	220	1318
18,50498	167	1265,5
19,50533	129	1228
20,50566	102	1208
21,50601	93	1199
24,50706	174,5	1268
27,50808	408	1483
29,50876	611	1701
31,50940	901	1973
35,51070	1640	2689,5

117

118

119



120

121 **Figure 2.** The Southern limb of the Sun over 220 mark of the meridian line on 21st December 2020.
122 The reddish penumbra is 5 mm thick, and limb darkened. On right side a paper meter with cm and
123 mm marks.

124 2.2.3 Perihelion influence on the solstice's data

125 Being the perihelion in the first days of January (the 2nd in 2021) the angular velocity of the Sun with
126 respect to the "fixed" stars reaches a maximum at that date. This shifts the meridian transit about 30
127 seconds ahead each day (true solar day of 24 h 30 s), but also the velocity of declination's motions is
128 asymmetric with respect to the solstice, being larger around perihelium. A simple quadratic fit
129 points to a minimum which is before the actual one. This effect is reduced when the fit's dates are
130 closer to the solstice (17-24 December) yielding the "tropic" at 10:52 TMEC, only 10 minutes before
131 the ephemerides, but with a larger uncertainty of ± 48 minutes, owing to the lack of data on 22 and
132 23 December (clouds). See also section 2.3.3 on the duration of SGR and CAP signs.

133 2.2.4 Obliquity secular variation (1700-2020)

134 The Southern limb position of the Sun for the 2020 winter solstice was 95.6 mm before the end of
135 the meridian line, or 42.4 mm after the 220 mark. Since that day the passage occurred 45 mm after,
136 there is a difference of 2.6 mm between the observation and the fit and this is due to local
137 meteorological effects (more refraction implies a higher image, and a lower position on the
138 meridian line). For the 21st of December this difference is corresponding to about 5". This can be
139 considered as a typical *Bianchini effect*, due to atmospheric refraction on the 21st of December 2020.
140 This value has been obtained only from the parabolic fit of the positions measured on the meridian
141 line, it is not a consequence of a systematic error in the calibration of the meridian line. The
142 backwards movement of the solstice Southern limb due to Earth's obliquity variation has been 85.6
143 mm since 1700 (from the black border of the Capricorn, 10 mm thick), so 0.2675 mm/yr or 0.474"/yr.

144

145 **2.2.5 Nutation measurement for 2020 winter solstice**

146 The evaluation of the nutation effect for 2020 depends on the calibration of the present meridian
147 line-pinhole. In other words the end of the meridian line corresponds to a distance from the base of
148 the pinhole (the vertical of its center). Here we assume 44916.9 mm this reference distance, and the
149 astronomical data offer the possibility to correct it. The altitude of the pinhole is 20353.44 mm [6].

150 To obtain the current value of ε , the obliquity, for 21st December 2020 on the solstice's day, the
151 effective pinhole's center should have been shifted of 2.35 mm Northward.

152 This pinhole's shift toward North corresponds to shrink the reference length of the meridian line of
153 2.35 mm. The same result would be obtained by raising the pinhole's altitude by 1.08 mm, leaving
154 fixed the meridian length.

155

156 **2.2.6 The penumbra effect and the sharpness of the solar image**

157 The image of the Sun is generated by a pinhole. There is no lens to focus it. This is an advantage on
158 large angular measurements, over 47° of meridian altitude from winter to summer solstice.
159 The absence of a lens eliminates all optical distortions. But the image of the Sun is not with sharp
160 edges, though there is a preferred distance at which the diffraction's "pixel" $F\lambda/D=D$ equals the
161 pinhole projection.

162 Because of the (unwanted) cylindric geometry of the pinhole it happened during two solar rotations
163 (November and December 2020) to observe the AR 2786, a large solar spot, with a good imaging
164 precision.

165 This happened because the meridian projection of the pinhole (the effective pinhole, which is the
166 "pixel") was about 12 mm wide. A solar spot of this angular dimension (12 mm at 50000 mm of
167 distance, 48") could and has been seen. Similarly the limb of the Sun was visible with the same
168 resolution, and the penumbra effect was limited to this dimension.

169 Since the limb of the Sun is subjected to the limb darkening function, due to the solar atmosphere, it
170 happens that both penumbra and limb darkening act to reduce toward the center of the image the
171 perceived position of the limb of the Sun. At the eye the solar limb appeared redder as reflected
172 from the white marble "Imetto" [4] when the sky was completely clear.

173 Either in case of hazy or clear sky the penumbral effect has been evaluated by comparing the
174 measured diameter, obtained by the time duration of the transit $\Delta t \cdot \cos(\delta) \cdot 15''/s$ and the solar
175 diameter from the ephemerides.

176 The percentual of pinhole diameter corresponding to the enlargement of the diameter due to the
177 penumbra is between 30% to 50%, and even more. Bianchini chosen 50%, Eustachio Manfredi in
178 Bologna [5] was more oriented toward 100%, most probably because of prevalence of hazy weather
179 (for which also in Rome we measured larger values of penumbral effect).

180 Penumbral effect is symmetrical at Northern and Southern limbs, so the center is rather unaffected
181 by it. The estimate of the obliquity by using only one of the limb positions would include this
182 random meteorological effect of penumbra.

183

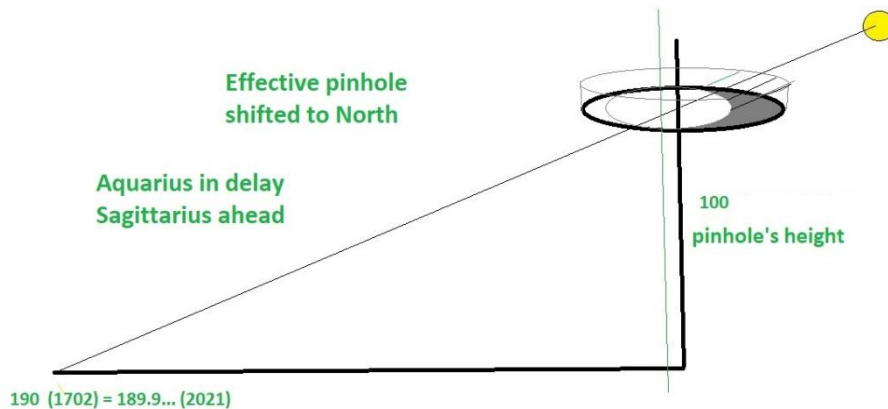
184 2.3. Calibration of the current pinhole with the Sagittarius – Aquarius signs

185 The pinhole has been modified since the original one of Francesco Bianchini. In the year 2000 we
186 found an irregular pinhole about 40 x 15 mm. Now, since 27 October 2018, a circular pinhole of 25
187 mm diameter and 6.11 mm thick is in place. The thickness determines a seasonal change of the
188 effective aperture and of the effective center of the pinhole, with the meridian solar altitude's
189 change [Figure 3]. The present diameter is slightly larger than the original (20 mm). The position of
190 its center is not the same of 1702, and has been calibrated.

191 2.3.1 The effective pinhole

192 The cylinder's shadow of the pinhole shifts its effective center (of the illuminated part) 7.1 mm
193 toward North at the Aquarius/Sagittarius limit. The maximum effect occurs, obviously, at the
194 winter solstice and it is 8 mm.

195 The pinhole shift of 2.37 mm Northwards found at the Aquarius/Sagittarius limit, to obtain the
196 corresponding solar declination, is a shift of the effective pinhole, the barycenter of the opened
197 surface.



198

199 **Figure 3.** Shifting the pinhole along the meridian line, and the shadow's effect of the cylinder.

200

201 2.3.2 The ingress in Sagittarius and Aquarius (SGR and AQR)

202 The ingress in Sagittarius and Aquarius has been used to know the displacement of the pinhole
203 with respect to the meridian line's reference marks. This measurement is somewhat similar to the
204 ones at the equinoxes, with a three times space resolution, being the solar image 900 mm long, in
205 the range of the meridian equivalence $2''=1$ mm.

206 The Sagittarius/Aquarius enters at 188.24 centesimal parts, but the real/effective pinhole can be
207 shifted with respect to the zero of the reference marks. The Sagittarius ingress occurs with the

208 image of the Sun as shifted as the pinhole, and it reaches the sign with an anticipation or a delay
 209 [Figure 3]. For the Aquarius ingress, the Sun's image reaches the sign with a delay which should be
 210 exactly of the same amount of time of the anticipation found at the Scorpius/Sagittarius
 211 symmetrical situation. This happens in the Aquarius because the image comes from the Northern
 212 side of the meridian line, and it finds the limit Capricorn-Aquarius after the real ingress, the
 213 contrary occurs for the Scorpius-Sagittarius symmetrical limit.

214 **Table 3.** Symmetrical passages into Sagittarius and Aquarius: meridian positions of the solar limbs
 215 measured from the end of the line. The declination of the ingress in these zodiacal signs is -
 216 $20^{\circ}08'57.8''$ or $h=27^{\circ}58'44.1''$. Data about the ingress in Scorpius 2020 ($-11^{\circ}28'19.6''$) are also plotted.
 217 The position of the signs are computed for 20353.44 mm of pinhole's height and a meridian line of
 218 44916.9 mm of length, as measured by Cultrera et al. (2018) [6]. The Scorpius data will be analyzed
 219 when the symmetric Pisces ingress will be available.

Date	Southern limb [mm]	Northern limb [mm]
22 October 2020 12:54:37	17463,5	18003,5
23 October 2020 12:54:31	17123,5	17660,5
Libra/Scorpius		17569,43
Aquarius/Pisces		
21 November 2020 11:56:17.0	6301	7172,5
22 November 2020 11:56:35.0	5949	6834
Capricorn/Aquarius		6619,53
Scorpius/Sagittarius		
18 January 2021 12:20:49 ¹	5668	6576
19 January 2021 12:21:08.1	6018,5	6903,5

220 ¹ Solar limbs measured from a photo taken by Heike Baranowsky (thanks!) on the meridian line.

221 The Sagittarius' ingress was obtained on 21 November 2020 h 21:30, 10 minutes before the
 222 ephemerides; Aquarius' ingress is found on 19 January 2021 h 21:49, 10 minutes after the
 223 ephemerides, interpolating the 19th measure with the 20th simulation, because of clouds, the
 224 extrapolation 18th-19th brings to 36 minutes of delay because of the change in declination's velocity
 225 of the Sun. The positions of the borders Scorpius-Sagittarius and Capricorn-Aquarius are the same,
 226 because the obliquity of the ecliptic does not change in 2 months. The absolute time shifts are 10
 227 minutes for both signs; since the velocity of the image at that point of the meridian line is 350
 228 mm/day, there is a pinhole's shift (2.37 ± 0.02 mm North) of the effective pinhole with respect to the
 229 zero reference (1702 pinhole's vertical).

230 Conversely, leaving fixed the length 44916.9 mm and considering the height 20353.44 mm as free
 231 parameter we can obtain the same result by raising it of 1.26 ± 0.01 mm for the SGR/AQR limit and
 232 1.08 mm for the CAP solstice. Both shift give 1.17 ± 0.09 mm upwards which is in agreement with the
 233 typical errorbar of such geometric measurements.

234 2.3.3 The duration of the Sagittarius and Capricorn zodiacal signs and the perihelium

235 The duration between SGR and AQR ingresses has been nearly exactly 59 days, from 21st November
 236 2020 to 19 January 2021 at 21:40 TMEC both dates. In the middle of both dates, exactly, we would
 237 expect the solstice, which is the ingress in CAP, but it happened at 11 TMEC instead of at 9:40
 238 TMEC of 21 December, as it would be obtained by the average (and by the parabolic fit extended
 239 from November to January). This method was used by Nicolò Cusano (1401-1461) to measure the
 240 winter solstice. In reality at the meridian line we measured the durations of the signs as following:

241 SGR-CAP 29 days 13h 20 minutes and CAP-AQR 29 days 10 h 40 minutes.
 242 The difference is due to the perihelium which occurred in the CAP sign on January 2nd, 2021; the
 243 Capricorn is the “fastest” sign.

244

245 **2.3.4 The agreement between CAP solstice and SGR/AQR measurements**

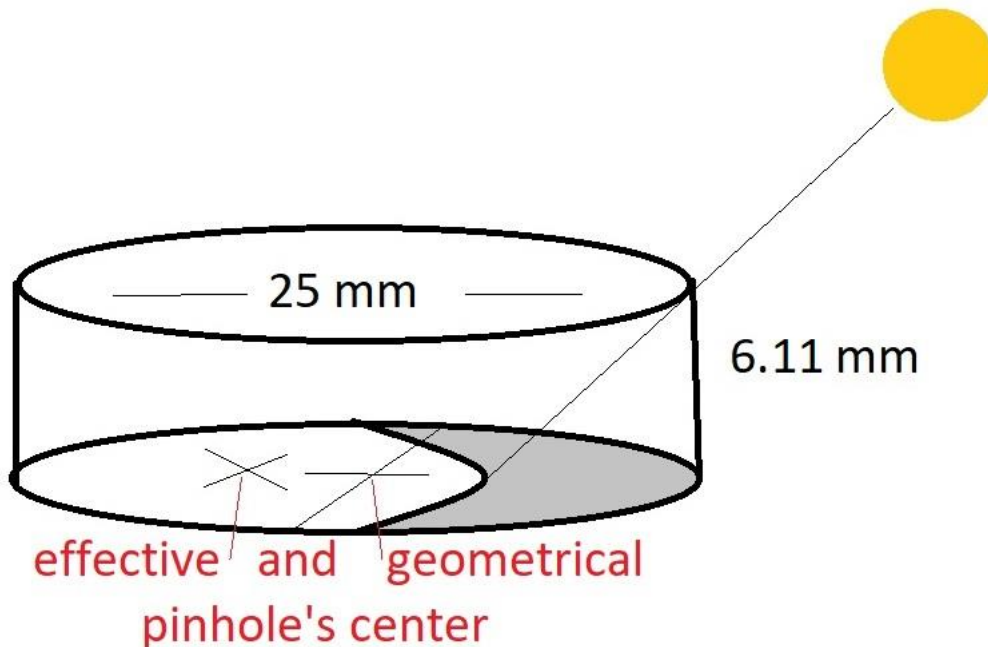
246 Knowing the shadowing effect of the cylindrical pinhole, for the winter solstice in Capricorn we
 247 have 13.28 mm of shadow and 6.64 mm of Northward shift of the effective pinhole due to this
 248 effect. Similarly for SGR/AQR the shadowing is 11.50 mm and the shift 5.75 mm North.

249 This shift is geometrical, calculated from the thickness of the cylindrical pinhole and from the solar
 250 meridian’s height. The full length of the meridian line is to be reduced by 2.36 ± 0.03 mm to account
 251 for the measurements of CAP, SGR and AQR ingresses. This reduction includes the aforementioned
 252 geometrical shadowing shift. Then we have two independent equations to obtain the pinhole axis
 253 shift with respect to the 1702 original positions (positive shifts are Northwards); these two
 254 equations have one incognita, so they can be used to find its errorbar.

255 $2.35 \text{ mm} = 6.64 \text{ mm} + X_v \text{ CAPshift}$ $X_v \text{ CAP} = -4.29 \text{ mm}$ (toward South)

256 $2.37 \pm 0.02 \text{ mm} = 5.75 \text{ mm} + X_v \text{ SGR/AQR shift}$ $X_v \text{ SGR/AQR} = -3.38 \text{ mm}$ (toward South)

257 Finally $X_v = -3.83 \pm 0.45 \text{ mm}$, which can be realistically written as $-3.8 \pm 0.5 \text{ mm}$ (toward South). A
 258 verification of this number was done with a plumb, in November 2018.



259

260 **Figure 4.** The effective pinhole and the shadow’s effect of the cylinder on the position of the center
 261 with respect to the axis.

262 The other possibility, more reliable on the point of view of errorbars, is the vertical shift of the real
 263 pinhole of $1.17 \pm 0.09 \text{ mm}$. In this case the two equations before become simply
 264 $6.64 \text{ mm} = X_v \text{ CAPshift}$ and $5.75 \text{ mm} = X_v \text{ SGR/AQR shift}$

265 because the shift is due only to the shadowing effect, and the axis of the present pinhole is the same
266 of 1702 (or the one referred to the zero of 44916.9 mm). Between these two possibilities is placed the
267 real situation, i.e. it is possible both a small meridian shift ≤ 3.8 mm South and a vertical one ≤ 1.2
268 mm. The future measurements and data analyses will clarify this result. About East-West shift it is
269 probably ≤ 6 seconds West on winter solstice, i.e. ≤ 19.8 mm, by using the solstices delays measured
270 by Boscovich in 1750 of 5 and 17 s, and the present ones 11 s and 23 s. The value of 6 s is to be
271 considered as an upper limit.

272 **2.4. Time measurements at the meridian line**

273 The technique of the video with a synchronized watch at the meridian line has been improved since
274 20 years. The scope is to have single photograms with absolute accuracy of 1/30 s or 1/60 s,
275 according to the video time acquisition. A single contact with the meridian line is affected by a
276 strong turbulence, enhanced by the opening of the pinhole, so the technique includes also parallel
277 lines measurements.

278 These lines were drawn on a paper sheet or, more recently, the marble lines 451 mm before and
279 after the bronze line, that were built exactly symmetric. The standard deviation of these time
280 averages is as good as 0.4 s. A single exceptional case there is the 1st May 2019, where the standard
281 deviation was 0.2 s because of a very cold weather outside and the Sun appeared just in the transit's
282 phase.

283 **2.4.1 The Eastward deviation between the solstices**

284 The global value of the deviation was estimated as 5' 11" Eastward, by averaging about 70
285 measurements in 2018 and 2019. This deviation corresponds with 11 s and 23 s of delay of meridian
286 passages in summer and winter solstices respectively. The deviation of the meridian line is larger
287 than the deviation from the true North of the small "boreal line" used with the Polaris during the
288 measurements of the latitude. Without radio-controlled watches Anders Celsius measured 2' in
289 1734 and Rudjer Joseph Boscovich 4.5' in 1750 (5 s and 17 s of delay at solstices).

290

291 **2.4.2 The Boscovichian sine**

292 Boscovich found also a further deviation of the line, local, up to 5 mm, from the line already
293 Eastward. It has been called Boscovichian sine because Boscovich speaks about a sine, described by
294 the residuals, along the meridian line. This sine has been individuated around the number 165, in a
295 very difficult zone for the measurements, because the line is among the benches of the church, and
296 the season is often rainfull.

297 To evidence this sine a new ephemerides has been published this year 2021, which includes the
298 global deviation of the meridian line between the solstices. The further deviation of 5 mm
299 corresponds to maximum 2 seconds of difference from this ephemerides and the observations (after
300 the average of the symmetrical contacts).

301 **2.4.3 The delay of Earth's rotation**

302 The availability of the measurements from 2018, with exactly the same setup (same pinhole, in the
303 same position) allows us to make comparison in the absolute transit's times and the ephemerides
304 (IMCCE, calsky, stellarium). Since the delay of the Earth's rotation in these years 2018 Oct-2021 Feb

305 did not exceed 0.3 s we do not see appreciable differences in the systematic delays between
306 ephemerides and observed transits. In 2009 after the introduction of a leap second at the end of the
307 year, this time shift was correctly observed.

308

309 **2.5. The orbit of the Earth and the meridian line**

310 The motion of the Earth acts on the positions of the Sun, which appears to circulate around the
311 Earth, and it is natural to use a circular orbit to represent it. The constant angular velocity does not
312 account for the variations of the Equation of Time, and since some centuries before Christ an
313 eccentric orbit has been used for the Sun. The orbit is traced at constant velocity, but the Earth is not
314 at its center, and this produces, along with the obliquity, a varying Equation of Time.

315 **2.5.1 Zodiacal signs**

316 The zodiacal sign are 12 equal parts of this circular orbit, which happens to be encompassed in
317 different time intervals: the Capricorn is the shorter one (see section 2.3.3 for our 2020-2021
318 measurements), because there is the perihelion inside, and the Cancer the longer one for containing
319 the aphelion. Each sign is related to the true obliquity ε and to the ecliptic longitude by the same
320 trigonometric formula, then its position depends on the epoch of the observation. On the meridian
321 line is fixed the value of the obliquity of 1701, which affects all signs but the equinoxes, which
322 remain unperturbed by the obliquity.

323 The reduction of the Capricorn limit was 128 mm in 3.2 centuries, then the reduction of
324 Sagittarius/Aquarius at 188.24 is 188.24/217.51 of 85.6 mm, say 74 mm. The Sagittarius/Aquarius
325 line now (2021) is shifted 74 mm toward the pinhole with respect to the position of the center of the
326 two symmetrical figures. With this approach (and not Stellarium computation for ecliptic longitude
327 300°) the Sagittarius/Aquarius limit is at 188.261 and the ingress in Aquarius was at 21:41 of
328 January 19 2021, in perfect agreement with Stellarium's timing. Conversely the Scorpius/Sagittarius
329 ingress was 8 minutes after the same ephemerides.

330 This section is essentially dedicated at the drawing of the meridian line and the signs, located with
331 a millimetric accuracy, being their geometrical center the limit of zodiacal signs computed for the
332 true obliquity ε of 1701.

333 The author of the zodiacal signs was Francesco Tedeschi, who replicated the maps of Johannes
334 Bayer (1703) with marble tarsie and brass star dimensioned according to their magnitudes.

335 **2.5.2 Earth's orbit eccentricity and consequences on the climate**

336 The ellipticity of Earth's orbit changes with the time because of the attraction of the other planets.
337 This parameter can be monitored at the Clementine Gnomon by knowing the "*anni cardines*" timing.

338 The Ptolemaic eccentricity is the distance, normalized to 1, between Earth's center and the solar
339 circular orbit's center. This value, by definition, is twice the eccentricity of the Keplerian ellipse of
340 the Earth's orbit.

341 That's why we have Earth's eccentricity observed values already two millennia ago. This is
342 important in celestial mechanics as well as in the climate studies, because a change in eccentricity,
343 in the apsis line, and the variations of the obliquity may act on climate change (Milankovitch

344 theory). From a relatively hot winters (at perihelion) for the Northern hemisphere, the opposite
345 situation is reached in about 5000 years with a cold winters (in aphelion) delaying the melting of the
346 snow (maintaining an high albedo).

347

348 **3. Conclusions**

349 The study on the meridian line of s. Maria degli Angeli, the Clementine Gnomon, made by
350 Francesco Bianchini in 1701-1702 and dedicated to the pope Clement XI (1700-1721), has been based
351 upon real observations of the Sun.

352 The summer solstice markers have been discovered in 2018 and discussed at IAU XXX General
353 Assembly. One of them is “blind” since 1750, after the intervenes of the architect Luigi Vanvitelli at
354 the Basilica for the Jubilee of that year, upon the will of pope Benedict XIV.

355 The first geometrical results has been the inclination of the great line with respect to the true North
356 between the solstices of 5' 11" Eastward. The smaller “boreal” meridian is about 2' Eastwards, more
357 precise than the larger one. This boreal line was realized at least 3 months before the Cardinal
358 Gianfrancesco Albani was elected pope (23 November 1700), in order to have the North-South
359 direction ready for 1-8 January 1701 when Bianchini measured the latitude by means of upper and
360 lower transit of the Polaris.

361 Francesco Bianchini and the ancient astronomers (Celsius and Boscovich are documented) used the
362 meridian line combining the timing of the Sun with the ones of the stars, both observed at the
363 meridian line. Nowadays we can observe only the Sun, and rely on the accurate calibration of the
364 meridian line (exact altitude of the pinhole, exact distance from the pinhole vertical projection).

365 Moreover a new pinhole, has been adapted to the meridian line on 27 October 2018, of diameter 25
366 mm, and a thickness of 6.11 mm which produces a meridian shadow variable with the season.

367 The positions of the markers on the meridian line from #37 to #220 has been measured with a total
368 station in November 2018 within some millimeters (1 to 4) of accuracy. New measurements
369 completed the calibration with astronomical observations, and the reference ephemerides were
370 Ephemvga (1992), Calsky (website working up to 2020) and Stellarium 0.20.2 (2020). All
371 measurements resulted within 10" from the ephemerides, but the Bianchini effect, due to the
372 meteorological conditions (Pressure and Temperature, mainly) was not clearly identified, until the
373 last winter solstice.

374 With the data of the 2020 winter solstice, treated in a parabolic fit, the present value of the obliquity
375 has been used to recover the fine adjustments to the pinhole's position and complete the
376 calibration. The accuracy to the nearest arcsecond for the obliquity ϵ has been possible because each
377 meridian transit has been obtained as the result of an average, to limit the air turbulence effect, and
378 this stated a precision of 1 mm for each transit, and the parabolic fit improved this accuracy to $1/\sqrt{N}$
379 where N is the number of days of observations. With 15 days of observations an accuracy of $\frac{1}{4}$ mm,
380 or 0.5" is possible, and it was effectively verified.

381 The instant of the solstice is affected by the asymmetry introduced by the perihelion 12 days after
382 the winter solstice. That's why this instant has been estimated by a few minutes of defect (10 to 20).

383 The study on the ingress in Sagittarius/Aquarius, calculated by linear interpolation between the
384 nearest meridian transits, offered new constraints on the actual pinhole position. The most reliable
385 result is a vertical shift of +1.2 mm, according to the typical instrumental errors for a total station,
386 and no meridian shift. The length of the meridian line from the pinhole base to the end is 44916.9
387 mm and the height is 20354.6 mm.

388 which is more dependent on the calibration of the meridian line, showed the possibility to obtain an
389 Bianchini affirmed to obtain in the timing of the “*anni cardines*” an accuracy within a few minutes
390 for the meridian (fully working with Sun and fixed stars). We were able to obtain a similar value
391 using only the positions of the Sun. The systematic error obtained in November and January is of
392 the same magnitude, even November datum was interpolated, and the January’s one was
393 extrapolated, slightly underestimating the meridian velocity of the image, then the further delay.

394 The published measurements show how to get an angular accuracy of 1 arcsec over a range of 47°
395 (difference in meridian altitude from winter to summer) which corresponds to a relative accuracy of
396 1 part over 170 000. If General Relativity was born on the side of Positional Astronomy (Mercury’s
397 perihelion precession), we are using the instrument where Positional Astronomy reached the
398 maximum accuracy for the “solar theory” after G. D. Cassini and before U. J. Leverrier and S.
399 Newcomb.

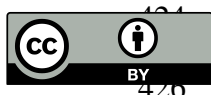
400 Stellar aberration (the first special relativistic effect) has affected the measures made by Francesco
401 Bianchini (1662-1729) at this meridian line for the latitude (1701 Polaris’ aberration) and the
402 seasonal meridian positions of Sirius (1701-2) and in the timings of “*anni cardines*”: the solstices
403 and the equinoxes of 1703 (difference between Sirius’ and constant solar aberration). The times for
404 the identification of the effect were about to come (1727, J. Bradley): the great Gnomon was affected
405 by systematic errors difficult to be “self” detected; our work is going in this direction.

406 **References**

- 407 1. F. Bianchini, De Nummo et Gnomone Clementino, Romae (1703)
- 408 2. C. Sigismondi, Lo Gnomone Clementino, Gerbertus 7, 1-78 (2014)
- 409 3. C. Sigismondi, <https://ui.adsabs.harvard.edu/abs/2008mgm..conf.2470S/abstract> (2008)
- 410 4. <https://www.isprambiente.gov.it/it/attivita/museo/collezioni-litomineralogiche/lito-reperti/marmo-imetto>
- 411 5. M. Catamo and C. Lucarini, Il Cielo in Basilica, Arpa Agami, Roma (2012)
- 412 6. G. Cultrera and P. Spera, First Report of Geometrical Measurements on the Clementine Gnomon, IIS Caffè,
413 Roma (2018)
- 414 7. http://neoprogrammics.com/nutations/Nutation_In_Obliquity.php
- 415 8. https://neoprogrammics.com/obliquity_of_the_ecliptic/Obliquity_Of_The_Ecliptic.php
416 (accessed on 25 January 2021).
- 417

418 **Acknowledgments** To don Franco Cutrone, pastor of the Basilica of Santa Maria degli Angeli e dei
419 Martiri in Rome, for the permission to work, measure, teach and film at the meridian line alone and
420 with many physics class of Secondary School, University and European Space Agency hundreds of
421 hours during many years, and for his request to present the results of these studies in a special
422 conference on the meridian line during the meridian transits of the “*anni cardines*” days.

423



© 2021 by the authors; licensee MDPI, Basel, Switzerland. This article is an open access article distributed under the terms and conditions of the Creative Commons by Attribution (CC-BY) license (<http://creativecommons.org/licenses/by/4.0/>).